Photoinduced Dissociation of Water and Transport of Hydrogen between Silver Clusters

Yu Zhang* and Jerry L. Whitten

Department of Chemistry, North Carolina State University, Raleigh, North Carolina 27695

Received: January 18, 2008; Revised Manuscript Received: April 8, 2008

Theoretical electronic structure calculations are reported for the dissociation of water adsorbed on a 31-atom silver cluster, Ag_{31}, and subsequent transfer of a H to a second Ag_{31} cluster leaving OH on the first cluster. Both ground and excited electronic state processes are considered for two choices of Ag cluster separation, 6.35 and 7.94 Å, on the basis of preliminary calculations for a range of separation distances. The excited electronic state of interest is formed by photoemission of an electron from one Ag cluster and transient attachment of the photoemitted electron to the adsorbed water molecule. A very large energy barrier is found for the ground-state process (3.53 eV at a cluster separation of 6.35 Å), while the barrier in the excited state is small (0.38 eV at a cluster separation of 6.35 Å). In the excited state, partial occupancy of an OH antibonding orbital facilitates OH stretch and concomitant movement of the negatively charged OH toward the electron−hole in the metal cluster. The excited-state pathway for dissociation of water and transfer of H begins with the formation of an excited electronic state at 3.59−3.82 eV. Stretch of the OH bond occurs with little change in energy (0.38−0.54 eV up to a stretch of 1.96 Å). In this region of OH stretch the molecule must return to the ground-state potential energy surface to fully dissociate and to transfer H to the other Ag cluster. Geometry optimizations are carried out using a simplex algorithm and a semigrid method. These methods allow the total energy to be calculated directly using configuration interaction theory.

1. Introduction

The production of hydrogen from water is being pursued on many fronts with the ultimate goal of producing a versatile and nearly unlimited fuel. Among these investigations are heterogenic processes on catalytic surfaces, homogeneous reactions involving transition metal complexes, and the design of biologically inspired catalytic systems. Since the overall reaction $H_2O \rightarrow {}^1/_2O_2 + H_2$ is endothermic, an energy source is required, and, for this purpose, sunlight would be very attractive if reasonable efficiencies could be attained.

In heterogeneous reactions involving the dissociation of gas-phase water on catalytically active transition metal surfaces, one can envision stepwise processes that successively remove hydrogen from water and transport the adsorbed H to other surface regions that favor H−H recombination rather than recombination to produce OH or H_2O. Success in harnessing these, yet to be discovered, steps will require a detailed understanding of the kinetics and energies of nonequilibrium processes.

In this study, we explore theoretically a well-defined photo-induced process in which a single hydrogen is dissociated from a water molecule adsorbed on a small Ag cluster (31 atoms) and transported through space to a nearby 31-atom Ag cluster. To assess the feasibility of the process, we need to know accurate values for critical geometries and energy barriers for both ground and electronically excited processes. This requires calculations using a high-level many-electron theory in which electron correlation is properly included in both ground and excited electronic states. For this purpose, we use the full many-electron Hamiltonian for the electronic structure problem, introduce core−electron pseudopotentials for silver, and construct wave functions by configuration interaction, i.e., a many-electron ab initio approach as opposed to density functional theory (DFT). Since the cross-section for photon absorption is larger for the metal cluster than for the adsorbed water molecule, we consider the process to be equivalent to an electron attachment reaction in which a photoemitted electron of silver transiently attaches to an adsorbed water molecule. The electronic state that results can be viewed as an electron-transfer excited state of the H_2O−metal cluster system. This photoinduced excited state can evolve on the excited-state potential energy surface or return at some point to the ground-state surface and undergo further reaction because of excess vibrational energy. Energy barriers will determine whether a viable process exists in which H can be released and transported to the other surface.

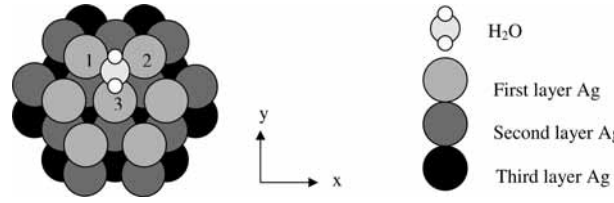

Figure 1. Top view of the fcc site studied for H_2O adsorption/dissociation on the Ag(111) surface of the Ag-31 cluster. Radii of the silver atoms are shown at reduced size for clarity of visualization.

2. Cluster System and H-Transfer

A cluster of 31 Ag atoms in a fcc structure is chosen to represent one of the nanoparticles; there are seven Ag atoms in the (111) first layer and 12 Ag atoms in both the second and third layers. A schematic representation of the geometry of a H_2O molecule adsorbed at a fcc (hollow) adsorption site on the first layer of the cluster is depicted in Figure 1. The Ag−Ag distance is set at the experimental bulk value, 5.46 au (2.89 Å). The three Ag atoms in the first layer (labeled 1−3 in Figure 1)

* To whom correspondence should be addressed.

10.1021/jp800528j CCC: $40.75
Published on Web 06/25/2008

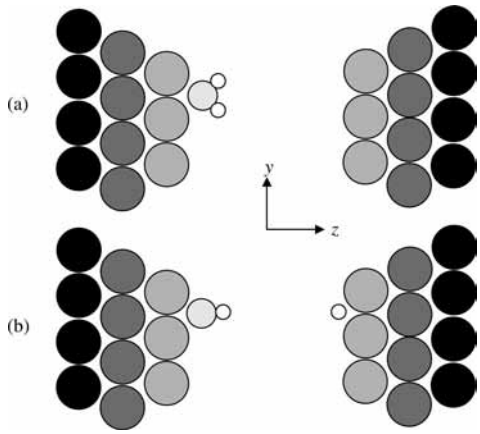

Figure 2. Dissociation of water and transfer of hydrogen between silver clusters. Schematic side view of the initial (a) and final (b) geometries of the two-cluster system. See also Figure 1.

which directly bond to H_2O are described by a 28-electron−core potential with 4s, 4p, 4d, and 5s electrons outside the core. The latter, valence electrons are described by 4s, 4p, 4d′, 4d″, 5s′, 5s″, and 5p basis functions. All other silver atoms have a 46-electron−core and 5s′, 5s″ basis functions. The hydrogen atoms are described by 1s′, 1s″, and p functions, and oxygen has five s-type functions and two p-type functions plus a set of d-polarization functions. The basis is large enough to ensure near Hartree−Fock quality atomic solutions. The additional basis functions allow orbitals to polarize in a molecular environment and permit correlation excitations to the next atomic shell.

A second Ag cluster, identical to the first cluster, is positioned in mirror symmetry at a set distance of either 12 (6.35 Å) or 15 au (7.94 Å). These two choices of the cluster separation distance were based on preliminary calculations carried out for separations ranging from 9 (4.76 Å) to 15 au (7.94 Å). The calculations, even though the geometries were not fully optimized, show a decreasing ground-state barrier to H-transfer when the cluster separation distance is decreased. At the closest separation distance considered, the H in a slightly stretched OH bond can directly interact with the other cluster. At the separation distance of 15 au, the ground-state barrier to H-transfer is almost identical to the barrier of H-transport away from the water molecule into the space in a single-Ag-cluster system, which indicates that there is little interaction between the second Ag cluster and the dissociated water molecule at this separation distance. The two-cluster system is depicted in Figure 2. The initial geometry with H_2O adsorbed on the left Ag cluster is shown in Figure 2a, and the final geometry after a H-transfer to the right Ag cluster is shown in Figure 2b. The objective of the present work is to consider photoinduced dissociation of water that leaves OH on the left cluster and allows H-transport to the right cluster. At each step in the transfer of H toward the other cluster, both ground and electronically excited states are calculated in order to determine the energy barrier for each potential energy surface.

3. Theory and Method

The water−silver cluster system is described in the present work by an embedded cluster method that is designed to give an accurate many-electron description of the adsorbate−surface region. Many applications of the method to ground and excited states of adsorbates on metals have been reported previously, and details of the method can be found in refs 1–3. There are two distinct components of the embedded cluster method described in the references cited above, boundary conditions on the cluster itself that appropriately couple the cluster to a larger bulk system and the localization transformation that defines the electronic subspace treated by configuration interaction. In the present work, since we are interested in small, 31-atom, silver clusters, no cluster boundary conditions are employed, and the terminology "embedding" refers only to the creation of a subspace that is treated by configuration interaction. A brief summary of the main elements of the approach is given below.

Calculations are carried out for the full electrostatic Hamiltonian of the system (except for core−electron potentials), and wave functions are constructed by self-consistent-field (SCF) and multireference configuration interaction (CI) expansions,[4–6]

$$\psi=\sum_k c_k \det(\chi_1^k,\chi_2^k,...,\chi_N^k,...,\chi_n^k)$$

The Hamiltonian, including atomic core potentials, V^{core}, is of the form

$$H=\sum_i^N\left(-\frac{1}{2}\nabla_i^2+\sum_k^Q\frac{-Z_k}{r_{ik}}\right)+\sum_{i<j}^N\frac{1}{r_{ij}}+\sum_i^N V_i^{\text{core}}$$

where

$$\langle a(i)\left|V_i^{\text{core}}\right|b(i)\rangle=\langle a(i)\ b(i)\left|1/r_{ij}\right|\rho(j)\rangle-\langle a(i)\ b(i)\left|1/r_{ij}\right|\gamma(i,j)\rangle+\sum_m\lambda_m\langle a(i)|Q_m(i)\rangle\langle Q_m(i)|b(I)\rangle$$

and ρ, γ, and Q_m denote atomic densities, exchange functions and core atomic orbitals, respectively. This type of effective core potential and basis construction, discussed in ref 5, maintains rigorous orthogonality of valence and core basis functions on the same nucleus.

Initial variational energy minimization calculations are carried out at the single-determinant, SCF level. The occupied and unoccupied SCF orbitals are then localized separately to maximize their interaction with the adsorbate and the metal atoms of the adsorption sites. Highly localized orbitals are used to define the CI active space. Finally, the CI wave function, ψ, is generated from the dominant SCF configuration, ψ_0, plus other important configurations by single and double excitations:

$$\psi=\psi_0+\sum_k C_k\psi_k$$

The initial representation of the excited state is obtained from the following sequence of calculations: (a) SCF calculation of the ionized system $H_2O/Ag(111)^+$; (b) localization of the virtual SCF orbitals about H_2O and surface Ag atoms (using exchange maximization), removal of transformed virtual orbitals that do not contain appreciable H_2O character; and (c) SCF calculation of the electron-attached excited state corresponding to electron excitation from Ag(111) to H_2O. The resulting representation of the state is defined as ψ_0.

All configurations, ψ_k, are retained if an interaction threshold

$$|\langle\psi_k|H|\psi_0\rangle|2/(E_k-E_0)>2\times10-7\text{ au}$$

is satisfied. Contributions of excluded configurations are estimated using second-order perturbation theory.

4. Results and Discussion

4.1. H and OH Adsorption. We first examine the adsorption properties of H (Figure 2b right cluster) and OH (Figure 2b left cluster) separately; both adsorbates are at fcc hollow sites on the Ag(111) face. The calculated equilibrium adsorption

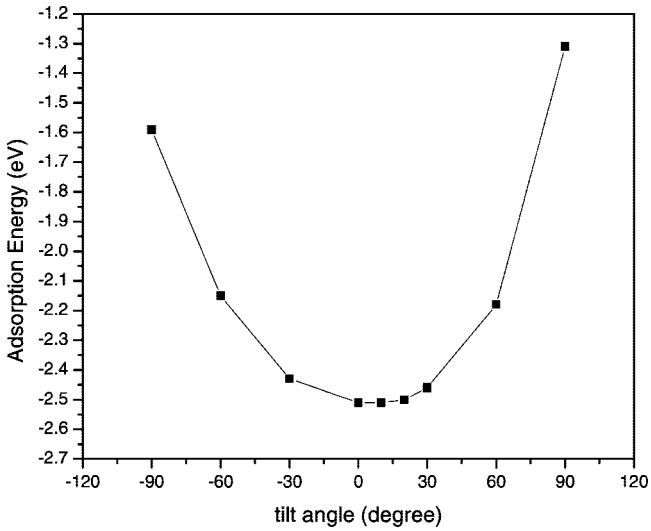

Figure 3. Adsorption energy versus tilt angle of OH at a fcc hollow site on the (111) face of the Ag_{31} cluster. The tilt angle is defined as the angle between the OH axis and the surface normal. The O to Ag surface distance and OH distance are 3.1 au (1.64Å) and 1.84 au (0.97Å), respectively.

energy and H to Ag surface distance are 2.02 eV and 2.2 au (1.16 Å), respectively. For OH, the adsorption energy and O to Ag surface distance are found to be 2.51 eV and 3.1 au (1.64 Å); the O−H bond length is optimized at 1.84 au (0.97 Å). The adsorption energy for OH at different angular orientations in a plane perpendicular to Ag surface (the *yz* plane in Figure 2) is shown in Figure 3.

The optimum tilt angle between the OH axis and the surface normal is found to be 0°; however, the potential curve is very flat near the energy minimum. There is only a small decrement (≤0.08 eV) in adsorption energy from 0 to ±30°, compared to a 1.20 eV decrement from 0 to 90°.

4.2. H_2O Adsorption. The equilibrium geometry of H_2O adsorbed on the Ag(111) face is optimized by using an optimization program based on the Nelder−Mead simplex method.[7,8] This is an effective minimization method since the potential energy surface is determined directly at the CI level. Six variables are chosen in the minimization: the O−Ag surface distance, the OH bond length, and four angles (two angles for each OH in spherical coordinates). Three high-symmetry adsorption sites of the surface, atop, bridge and fcc hollow are considered, and the energy minimum has been found for each site. The optimized geometries corresponding to the energy minima are depicted in Figure 4. In Table 1 we tabulate the adsorption energies and the geometrical parameters of H_2O.

We find the fcc hollow site configuration is the global energy minimum, and the calculated adsorption energy of 0.24 eV is indicative of a rather weak interaction between water and silver. The H_2O molecular plane is perpendicular to the (111) surface with the two OH axes forming angles of 22.5 and 82.5° with respect to the surface normal (as shown in Figure 4). The adsorption energies for the atop and bridge sites are 0.14 and 0.19 eV, which are slightly less than at the fcc hollow site, and the H_2O molecular plane is more nearly parallel to the Ag surface, especially at the bridge site. In all three cases, as shown in Table 1, the optimized OH bond length *d*(OH) and bond angle ∠(HOH) are found to be close to the experimental gas-phase molecular geometry of 0.964 Å and 103.8°. The perpendicular orientation of the H_2O molecular plane relative to the Ag surface differs from the optimum geometry found in a high-quality periodic DFT calculation of water on Ag(111), where the

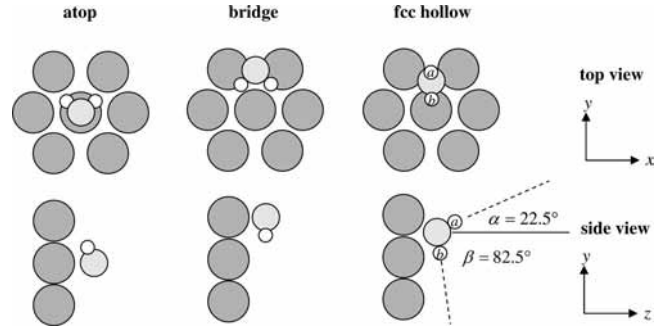

Figure 4. Optimized geometry of H_2O adsorption at atop, bridge, and fcc hollow adsorption sites on the (111) face of Ag_{31}. Only the top layer of Ag atoms is shown. The H, O, and Ag atoms are depicted as in Figure 1. Two H atoms at the fcc hollow site have been labeled as a and b. Parameters α and β are defined as the angles between O−H*a*, O−H*b* axes and the surface normal *z*-axis, respectively.

TABLE 1: Adsorption Energy and Structural Parameters of H_2O Adsorbed at Different Sites on the (111) Face of a Ag_{31} Cluster. Results are from CI calculations[a]

site	E_{ads} (eV)	θ (deg)	∠(HOH) (deg)	*d*(OH) (au)	*d*(O−Ag surface) (au)
atop	0.14	124	102	1.86 (0.98 Å)	6.56 (3.47 Å)
bridge	0.19	85	100	1.85 (0.98 Å)	5.70 (3.02 Å)
fcc hollow	0.24	0	105	1.84 (0.97 Å)	5.54 (2.93 Å)

[a] Tabulated are the adsorption energy, E_{ads}; the tilt angle of the H_2O molecular plane with respect to the Ag surface normal, θ; the bond angle, ∠(HOH); the OH bond length, *d*(OH); and the distance between the O and Ag surfaces, *d*(O−Ag surface).

molecular plane for water at an fcc hollow site was found to be tilted 104° with respect to the surface normal.[9] Since water is very weakly adsorbed on the Ag surface and the change of adsorption energy in the DFT calculation is only 0.09 eV in going from perpendicular to a 104° tilt, the difference could be attributable to differences in theoretical method. In view of the small change in total energy in both calculations, we agree with one of the main conclusions of the earlier work that the orientation of coadsorbed water molecules would be determined by dipolar interactions and the opportunity of lone pair oxygen orbitals to hydrogen bond with a neighboring water molecule. At higher coverage, both of these effects should favor a structure with the H_2O plane more nearly parallel to the surface.

4.3. Dissociation of H_2O and Transfer of H. The task of finding the energy barrier for transfer of H, dissociated from water adsorbed on one silver cluster, through space to the other cluster could, in principle, require extensive geometry optimization. We note, however, that at the global minimum for water on silver (see Figure 4 fcc hollow site) one of the OH bonds (O−H*a*) forms an angle of 22.5° with respect to the surface normal, and this angle is already close to the optimum orientation of OH adsorbed at the same site. As shown in Figure 3, the adsorption energy change is less than 0.08 eV on changing the angle from 0 to ±30°. These facts suggest that a rather coarse grid of points will reveal the main features of the potential energy surface. In Figure 5, we show the schematics of such a grid calculation in which the O−H*a* bond length and orientation are fixed at their initial values in water and H*b* is moved in steps toward the other silver cluster. Following these calculations, the simplex method is used to refine the optimum geometrical parameters of the transition state.

The process described in Figure 5a begins with water adsorbed on one Ag cluster at a geometry corresponding to the global energy minimum for water on silver. In the initial grid calculation, the O−H*a* bond length and angle are fixed at 1.84

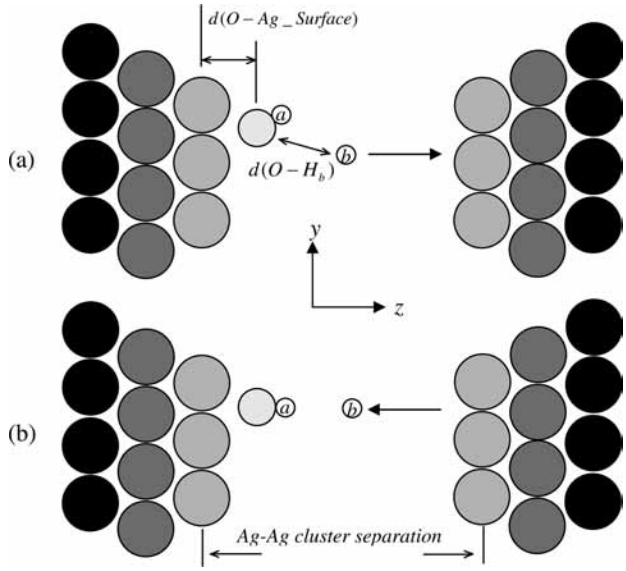

Figure 5. Dissociation of water and H-transfer between silver clusters. Grid calculations start at initial configuration (a) and proceed to a final configuration (b). The representation of H, O, and Ag atoms is the same as in Figure 1.

au (0.97Å) and 22.5° to the surface normal, respectively. The O to Ag surface distance (O−Ag surface) and the O to H*b* distance (*d*(O−H*b*)), are chosen as independent variables, and hydrogen, H*b*, is moved to the right cluster along the *z* direction. The opposite process is described in Figure 5b. The initial configuration is that of dissociated OH + H where OH*a* and H*b* are at fcc hollow sites on different Ag_{31} clusters, as shown in Figure 2b. The variables are the same as in Figure 5a, but H*b* is now moved in the $-z$ direction to reform a water molecule adsorbed on the left cluster. In these calculations, the *x* and *y* coordinates which have a negligible effect on the energy are unchanged during the transfer of hydrogen. Although seemingly redundant, proceeding in the forward and reverse directions is helpful to identify electronic states of different symmetry or charge distribution. Calculations are carried out for two different choices of Ag cluster separation: 15.0 (7.94 Å) and 12.0 au (6.35 Å) measured from the surface plane of nuclei in each cluster. The calculated ground-state energy versus *d*(O−Ag surface) and *d*(O−H*b*) parameters is shown in Figure 6; solid and hollow symbols are used to represent curves obtained from the initial, H_2O, starting point and from the OH + H end point, respectively.

We first note when the Ag cluster separation is at 15.0 au, as shown in Figure 6a, solid symbol curves, there is a very large increase in ground-state energy, ∼3.6 eV, when *d*(O−H*b*) increases from 1.84 to 3.0 au. However, the energy changes only slightly for O to Ag surface distances in the range of *d*(O−Ag surface) = 5.5−4.0 au. When *d*(O−H*b*) is increased further into the 3.0−5.0 au range, a much larger variation in energy with the O−Ag surface distance is found, and the lowest energy is for *d*(O−Ag surface) = 3.1 au. The energy barrier is 3.89 eV at *d*(O−H*b*) = 3.7 au. These facts indicate that, in the early stages of dissociation, H*b* is still tightly bound to O and H*a*−O−H*b* can be treated like a distorted water molecule; the small variation in ground-state energies for different *d*(O−Ag surface) in this region is due to weak interaction between water and the Ag surface. After the O−H*b* bond is nearly broken, the system moves to a lower total energy by dragging O−H*a* toward the Ag surface and forming a strong surface−OH bond. The final geometry, where the O to Ag surface distance is 3.1 au, is the same as for an OH adsorbate at the fcc hollow site on Ag(111), as discussed in section 4.1. Once the barrier is overcome, the total energy steadily decreases to the final configuration route, as shown by the hollow symbol curves.

Comparing the forward and reverse processes, it is found that the OH + H → H_2O reverse route (hollow squares) is about 1 eV lower in energy at *d*(O−H*b*) = 5.0 au than that given by the forward process (solid squares). This is a surprisingly large difference that is outside the range that could be attributed to details of convergence. Further examination shows that the wave functions at the two points have very different charge distributions and different symmetries for one of the higher occupied orbitals of the Ag clusters; thus, the points correspond essentially to two different states. The state produced in the forward process maintains a neutral Ag_{31} cluster on the right. In contrast, the reverse process produces a state in which the right cluster is +0.5|e| positive. In this configuration (Figure 5b), H*b* attracts electron density from the right Ag cluster. At the stretched distance, H*a*−O−H*b* has a net charge of −1|e| for both processes. Interestingly, these observations mean that as the H-transfer takes place, the H can serve as a bridge that allows electron transfer between the clusters.

Results for the smaller separation distance between Ag clusters, 12.0 au, show similar behavior. The ground-state total energy curves for forward and reverse processes are shown in Figure 6b. A lower energy barrier of 3.53 eV is found for the smaller separation distance. The route with the lowest energy is at *d*(O−Ag surface) = 5.5 au, which means that when the O−H*b* bond is broken, unlike in Figure 6a, the system will keep the O−H*a* between the two clusters instead of dragging it toward the left Ag surface. That is, if the O−H*b* bond is broken and the two Ag clusters are close enough, the system will move to a lower energy by either forming a bond between O−H*a* and the left Ag cluster or forming a bond between H*b* and the right Ag cluster. The competition between these possibilities leads to the different properties shown by the energy curves in Figure 6a,b.

The optimum geometry of the transition state at *d*(O−H*b*) = 3.7 au have been refined by using the simplex method in which *d*(O−H*a*), *d*(O−Ag surface), and the α angle between O−H*a* and the surface normal are chosen as the variables. Barriers with slightly lower energy of 3.55 and 3.25 eV are found for both Ag cluster separations at 15.0 au and 12.0 au, respectively. Since the decrements of the energy barrier are only ∼0.3 eV, which are less than 9% of the barriers obtained by the grid of points calculations, we conclude that the grid method has revealed the main features of the potential energy surface.

Excited electronic states that involve a change in the electronic structure in the water region of the system have been calculated as a function of geometry. These states are often referred to electron attachment states and can be viewed as a transient attachment of a photoemitted electron to the water adsorbate. The state formed initially in such a process has the same geometry as water in its ground electronic state. There are many other electronic states at lower energy corresponding to metal−metal excitations, but these states have essentially no effect on the dissociation of water. As described in the theory section, these states are isolated from the states of interest. Excited-state energies are presented in Figure 7 for the initial dissociation of H_2O and subsequent movement of H toward the other cluster. The lowest energy pathway for the ground state is shown as a dotted line for comparison. Excitation energies to produce the electron attached excited states are calculated to be 3.59 and 3.82 eV for Ag cluster separations of 15.0 au and 12.0 au, respectively. Once formed, it is possible to stretch the

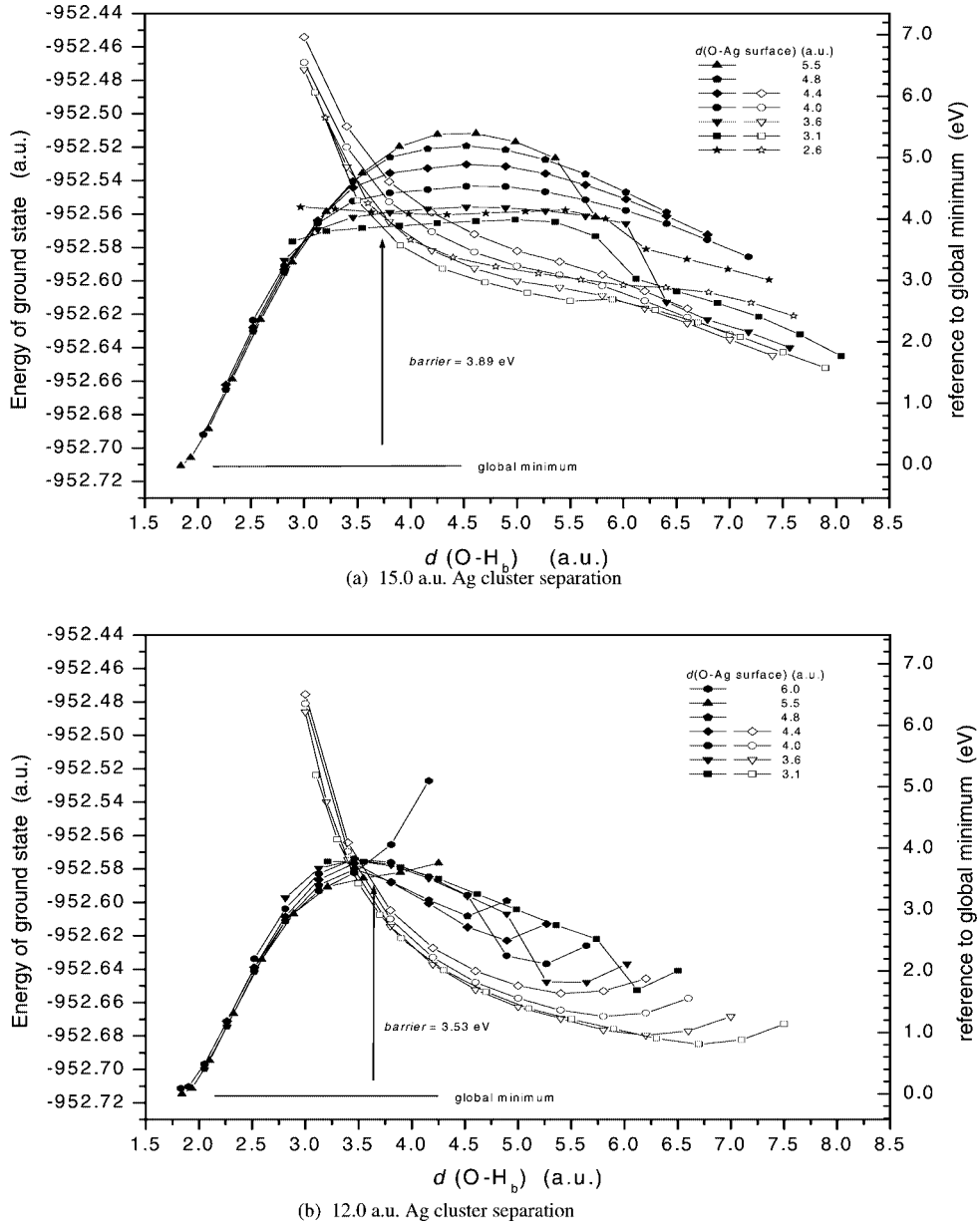

Figure 6. Ground-state energy for H_2O dissociation and H-transfer. Forward (a) and reverse (b) processes are shown, and points are indicated by solid and hollow symbols, respectively.

H···OH bond with little change in total energy. This is due to the nature of the electron attached state where excitation from Ag can be thought of as transiently occupying the H*b*−OH antibonding σ molecular orbital. The negatively charged water is stabilized by the hole in the metal which localizes near the water adsorption site. It follows that the interaction between O and H*b* is much weaker than in the ground state and a much smaller change in energy occurs on the H*b*−OH stretch. Figure 7 shows that it is possible to stretch the H*b*−OH bond to a distance of 3.7 au with an increase in excited-state energy of only 0.54 eV (15 au cluster separation, Figure 7a) and 0.38 eV (12 au cluster separation, Figure 7b). Further stretching of the H*b*−OH bond is accompanied by a large increase in energy for both separation distances, as shown in Figure 7.

From these results, it is possible to identify a viable process that would lead to water dissociation and transfer of H to the second cluster. Beginning with water adsorbed on one silver cluster, the key steps are as follows: (a) photoexcitation to create the electron attached excited state; (b) stretch of one OH bond of water on the excited-state potential energy surface to a distance greater than that corresponding to the ground-state barrier (1.96 Å); (c) decay of the excited state back to the ground state on the other side of the ground-state energy barrier; (d) continued transfer of H, energetically downhill, to the second cluster on the ground-state potential energy surface.

Although it is interesting that the photoinduced reaction described above can occur at modest excitation energies, there are other questions or limitations that will determine the practical utility of the process. Among these are the relatively low cross-sections for electron attachment and the lifetime in the excited state required for sufficient H−OH stretch. To be a viable stage in a process to extract H_2 and O_2, removal of the H from adsorbed OH is required followed by recombination of adsorbed O atoms to produce O_2.

5. Summary

Theoretical studies of H, OH, and H_2O adsorption and dissociation on a (111) surface of a three-layer Ag_{31} cluster are

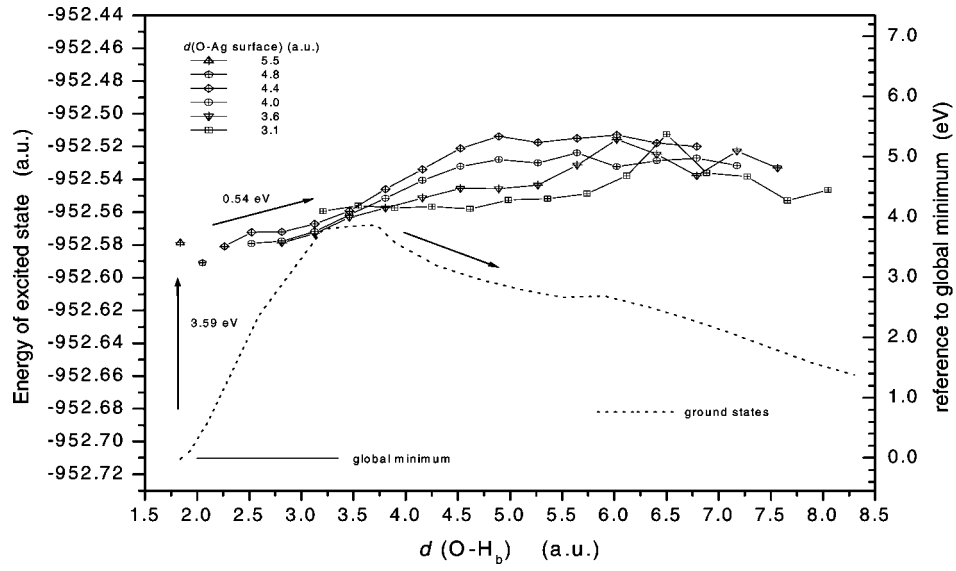

(a) 15.0 a.u. Ag cluster separation

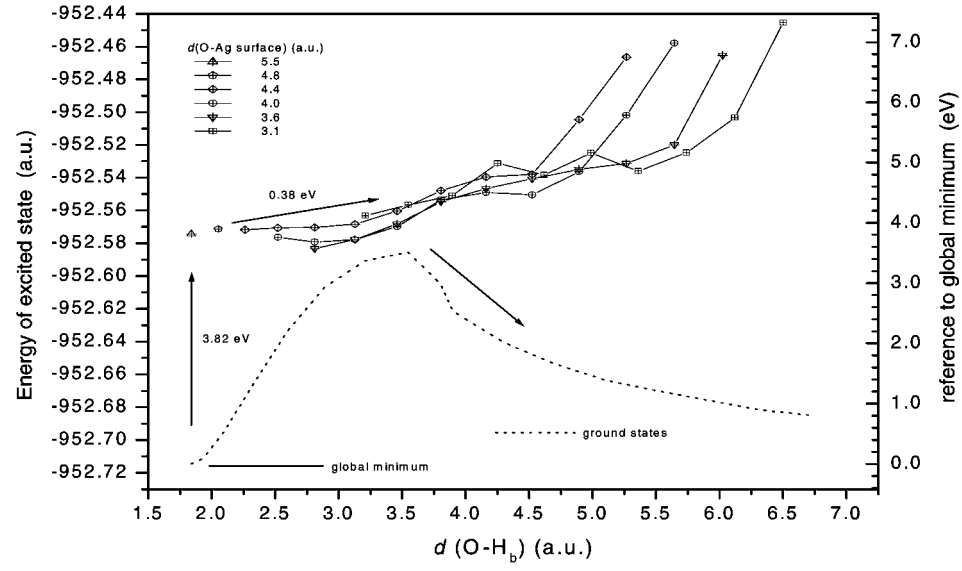

(b) 12.0 a.u. Ag cluster separation

Figure 7. Energy of excited electronic states during the dissociation of water adsorbed on a Ag_{31} cluster and H-transfer to the second Ag_{31} cluster. The dotted line represents the ground-state pathway for comparison.

reported. Following these studies, energy barriers for the transfer of a H from dissociated H_2O on one Ag cluster through space to a second nearby Ag cluster are calculated. Both ground and photoinduced excited electronic states are calculated. Results can be summarized as follows:

(a) H and OH adsorb at a fcc hollow site on the (111) surface of the Ag cluster; calculated adsorption energies are 2.02 and 2.51 eV, respectively.

(b) H_2O weakly adsorbs on the Ag(111) surface. At the fcc hollow site, the O-surface equilibrium distance is 5.54 au (2.93 Å) and the H_2O molecular plane is perpendicular to the Ag surface. However, the energy change on tilting the molecular plane to a geometry nearly parallel to the surface is small.

(c) In the ground state, the energy barrier for the transfer of a H to the other cluster is very high for both cluster separations that were considered, 3.89 and 3.53 eV at Ag cluster separations of 15.0 and 12.0 au, respectively.

(d) In the photoinduced excited electronic state corresponding to electron attachment to adsorbed water, the energy barriers for the transfer of a H to the other cluster are only 0.54 and 0.38 eV at Ag cluster separations of 15.0 and 12.0 au, respectively.

Acknowledgment. The authors thank the U.S. Department of Energy for support of this research.

References and Notes

(1) Whitten, J. L. *J. Chem. Phys.* **1993**, *177*, 387.
(2) Cremaschi, P.; Whitten, J. L. *Theor. Chim. Acta* **1987**, *72*, 485.
(3) Madhavan, P.; Whitten, J. L. *J. Chem. Phys.* **1982**, *77*, 2673.
(4) Whitten, J. L.; Yang, H. *Surf. Sci. Rep.* **1996**, *24*, 55.
(5) Whitten, J. L.; Yang, H. *Int. J. Quantum Chem.: Quantum Chem. Symp.* **1995**, *29*, 41.
(6) Sremaniak, L.; Whitten, J. L. *Surf. Sci.* **2002**, *516*, 254.
(7) Nelder, J. A.; Mead, R. *Comput. J.* **1965**, *7*, 308.
(8) Lagarias, J. C.; Reeds, J. A.; Wright, M. H.; Wright, P. E. *SIAM J. Control Optim.* **1998**, *9*, 112.
(9) Ranea, V. A.; Michaelides, A.; Ramirez, R.; Verges, J. A.; Andres, P. L.; King, D. A. *Phys. Rev. B* **2004**, *69*, 205411.

JP800528J